論文 / 著書情報
Article / Book Information

Title	Development of a Quenchbody for the detection and imaging of the cancer-related tight-junction-associated membrane protein claudin
Authors	Hee-Jin Jeong, Takuya Kawamura, Manami Iida, Yumi Kawahigashi, Mutsumi Takigawa, Yuki Ohmuro-Matsuyama, Chan-I Chung, Jinhua Dong, Masuo Kondoh, Hiroshi Ueda
Citation	Analytical Chemistry, Volume 89, Issue 20, Pages 10783-10789
Pub. date	2017, 10
Note	This document is the unedited Author ' s version of a Submitted Work that was subsequently accepted for publication in Analytical Chemistry, copyright (c) American Chemical Society after peer review. To access the final edited and published work see http://dx.doi.org/10.1021/acs.analchem.7b02047.
Note	This file is author (final) version.

Development of a Quenchbody for the detection and imaging of the cancer-related tight-junction-associated membrane protein claudin

Hee-Jin Jeong [a,‡,†], Takuya Kawamura [b,‡], Manami Iida [c], Yumi Kawahigashi [c], Mutsumi Takigawa [c], Yuki Ohmuro-Matsuyama [a], Chan-I Chung [a], Jinhua Dong [a,d], Masuo Kondoh [c], Hiroshi Ueda [a,*]

[a] Laboratory for Chemistry and Life Science, Institute of Innovative Research, Tokyo Institute of Technology, 4259 Nagatsuta-cho, Midori-ku, Yokohama, Kanagawa 226-8503, Japan

[b] Department of Chemistry and Biotechnology, School of Engineering, The University of Tokyo, 7-3-1 Hongo, Bunkyo-ku, Tokyo 113-8656, Japan

[c] Graduate School of Pharmaceutical Sciences, Osaka University, Suita, Osaka 565-0871, Japan

[d] Key Laboratory of Biological Medicine in Universities of Shandong Province; School of Bioscience and Technology, Weifang Medical University, Weifang, P.R. China

ABSTRACT: Claudins (CLs) are membrane proteins found in tight junctions and play a major role in establishing the intercellular barrier. However, some CLs are abnormally overexpressed on tumor cells, and are valid clinical biomarkers for cancer diagnosis. Here, we constructed antibody Fab fragment-based Quenchbodies (Q-bodies) as effective and reliable fluorescent sensors for detecting and visualizing CLs on live tumor cells. The variable region genes for anti-CL1 and anti-CL4 antibodies were used to express recombinant Fab fragments, and clones recognizing CL4 with high affinity were selected for making Q-bodies. When two fluorescent dyes were conjugated to the N-terminal tags attached to the Fab, the fluorescent signal was significantly increased after adding nanomolar-levels of purified CL4. Moreover, addition of the Q-body to CL4-expressing cells including CL4-positive cancer cells led to a clear fluorescence signal with low background, even without washing steps. Our findings suggested that such Q-bodies would serve as a potent tool for specifically illuminating membrane targets expressed on cancer cells, both *in vitro* and *in vivo*.

Tight junctions are essential cell-sealing complexes present between epithelial and endothelial cells and that provide a barrier to the diffusion of fluid via the intercellular space, thereby serving as determinants of paracellular permeability [1, 2]. Claudin (CL) is a tetra-transmembrane protein that forms the backbone of a tight junction and comprises a family consisting of 27 members that exhibit varying cell- and tissue-specific expression patterns and functions. CL plays a critical role in the maintenance of epithelial cell polarity and in controlling cell behavior, such as proliferation, differentiation, migration, and apoptosis [3-7]. Recent studies showed that CL overexpression is associated with cancer progression and metastasis [8]. CL3 and CL4 cover immune tissues, and their expression is up-regulated in ovarian, breast, prostate, pancreatic, and lung cancers[9-11], with CL1 expression and distribution also linked to cell-dissociation status in pancreatic cancer [12]. CLs are, therefore, considered valid clinical biomarkers for cancer diagnosis and also potent candidates for cancer-targeted therapy.

CLs can be readily detected via immunohistochemical methods, such as western blot and enzyme-linked immunosorbent assay, that utilize commercially available antibodies [6]. Despite their advantages of specificity and sensitivity, these methods sometimes return inaccurate results due to high background signals, as well as often being labor intensive and time consuming. Additionally, although single-photon emission computed tomography can be effectively used for CL imaging [13], the method requires a high level of technical expertise, as well as expensive equipment.

Here, we describe the development of Quenchbody (Q-body), a reagentless fluoroimmunosensor that can be used to quantify and image CLs. A Q-body is a site-specific, fluorophore-labeled antibody fragment that works on the principle of antigen-dependent removal of fluorophore(s) quenching by intrinsic tryptophan residues[14-23]. In the absence of antigen, fluorescence is quenched by photoinduced electron transfer from the tryptophan residues in the antibody to the fluorophore. However, when antigen is present, the bound antigen stabilizes the antibody conformation, thereby displacing the quenched dye surrounding the antigen-binding site, leading to de-quenching. Therefore, adding a Q-body to a target sample and measuring the associated increase in fluorescence allows antigen quantification within minutes, whereas most other conventional methods take several hours or days to obtain final results. As an antibody-based sensor, Q-body can detect not only small antigens, but also large antigens, such as proteins, and boasts a range of applications as a biosensor for many different types of antigens. However, to date, no attempts have been made to detect cellular-membrane proteins in vitro or in situ using Q-bodies. Here, we presented results

using a Q-body for the highly sensitive and convenient detection and imaging of CLs in solution and on cells (Scheme 1).

EXPERIMENTAL SECTION

Materials. The KOD-plus DNA polymerase was obtained from Toyobo (Osaka, Japan). Restriction enzymes and Escherichia coli SHuffle T7 Express lysY were obtained from New England Biolabs-Japan (Tokyo, Japan). Oligonucleotides were obtained from Operon-Eurofins (Tokyo, Japan). The PureYield plasmid miniprep kit was obtained from Promega (Tokyo, Japan). The In-Fusion HD cloning kit, Talon metal-affinity resin, and Talon disposable gravity column were obtained from Takara-Bio (Otsu, Japan). Ultrafiltration devices were obtained from Millipore (centrifugal filter tube Ultra-4, MWCO 3 k; Tokyo, Japan) or Pall (Nanosep Centrifugal-3 k; Ann Arbor, MI, USA). Immobilized Tris(2-carboxyethyl)phosphine (TCEP) disulfide-reducing gel was obtained from Thermo Pierce (Rockford, IL, USA). ATTO520-C2-maleimide (mal) was obtained from ATTOTEC (Siegen, Germany). Rhodamine 6G (R6G)-C5-mal was obtained from Setareh Biotech, LLC (Eugene, OR, USA). Tetramethyl-6-carboxyrhodamine (TAMRA)-C2-mal was obtained from Anaspec (Fremont, CA, USA). TAMRA-C5-mal was obtained from Biotium (Hayward, CA, USA). His-Sepharose Ni was obtained from GE healthcare (Piscataway, NJ, USA). Anti-DYKDDDDK-tag antibody beads and the DYKDDDDK peptide were obtained from Wako Pure Chemicals (Osaka, Japan). Recombinant CL4 protein was prepared using Sf9 cells infected with recombinant baculovirus[24]. Human colon carcinoma LoVo cells were obtained and maintained as described [25]. Other chemicals and reagents, unless otherwise indicated, were from Wako Pure Chemicals.

Gene constructions. VH of X (X=CL1-1, 2C1, or 3A2), which was cloned into pFUSEss-CHIg-hG1 (InvivoGen, San Diego, CA, USA), was amplified by polymerase chain reaction (PCR) using primers X_VHback and X_VHfor and KOD-plus neo DNA polymerase. VL of X, which was cloned into pFUSE2ss-CLIg-hk (InvivoGen), was amplified using primers X_VLback and X_VLfor. VH of Y (Y=4D3, 5A5, or 5D12), which was cloned into pUC118, was amplified using primers Y_VHback and Y_VHfor. VH of Y, which was cloned into pUC118, was amplified using Y_VLback and Y_VLfor. All primer sequences are provided in the Supporting Information Table S-1). CH1 with an N-terminal Cys-tag was amplified using primers hCH1XhoBack (5′-gtctcgagcgcttccacc-3’) and pUQ2_SOEnoLnkFor (5′-actagtctcattagagcattg-3’) and the Fab type Q-body expression vector pUQ2(KTM219)[16] as a template. The three PCR products were ligated by splicing by overlap extension PCR using primers X_VHback and pUQ2_SOEnoLnkFor. The product was inserted into *Age*I- and *Hin*dIII-digested pUQ2(KTM219) using an In-Fusion HD cloning kit, resulting in pUQ2(X). The obtained plasmid was prepared using the PureYield plasmid miniprep system, and the entire coding-region sequence was confirmed by sequencing.

Fab expression and purification. SHuffle T7 Express lysY cells were transformed with each expression vector and cultured at 30°C for 16 h in LBA medium (LB medium containing 100 μg/mL ampicillin) and 1.5% agar. A single colony was picked and grown at 30°C in 4 mL of LBA medium overnight, from which 1.6 mL was used to inoculate 100 mL of LBA medium. The cells were cultured at 30°C to an OD_{600} of 0.6, after which 0.4 mM isopropylthio-β-galactopyranoside was added. The solution was incubated for an additional 16 h at 16°C, followed by centrifugation (8000 g for 20 min at 4°C). The pellet was resuspended in 10 mL Talon wash buffer [50 mM phosphate, 0.3 M sodium chloride (NaCl), and 5 mM imidazole (pH 7.4)], followed by sonication. After centrifugation (8000 g for 20 min at 4°C), the supernatant was incubated with 0.2 mL of Talon metal-affinity resin on a rotating wheel for 30 min at 25°C, and the beads were washed three times with 25 mL Talon wash buffer. After addition of 4 mL Talon elution buffer [50 mM phosphate, 0.3 M NaCl, and 0.5 M imidazole (pH 7.4)] and incubation at 25 °C for 30 min, the eluent was collected using a Talon disposable gravity column. The eluent was subjected to an ultrafiltration device, equilibrated with PBST [10 mM phosphate, 137 mM NaCl, 2.7 mM KCl, and 0.05% Tween 20 (pH 7.4)], and concentrated to 250 μL. Protein expression and purification were confirmed by sodium dodecyl sulfate polyacrylamide gel electrophoresis (SDS-PAGE) analysis, and protein concentration was determined using various concentrations of bovine serum albumin (BSA) as a standard.

Fluorescence labeling and purification. A volume of immobilized TCEP disulfide-reducing gel slurry equal to the volume of 450 μg of purified protein was added to a microtube and centrifuged (100 g for 1 min at 4°C). After removing the supernatant, 450 μg of purified protein was added and incubated for 1 h at room temperature on a rotating wheel. After centrifugation at 100 g for 1 min, the supernatant was recovered and divided into four samples, with each reacted with a 20-fold mole of either ATTO520-C2-mal, R6G-C5-mal, TAMRA-C2-mal, or TAMRA-C5-mal in 2 μL dimethyl sulfoxide in the dark for 2 h at 25°C, respectively. Each reaction mixture was then incubated with 100 μL of His-Sepharose Ni beads on a rotating wheel at room temperature for 30 min. The beads were washed three times with 1 mL His wash buffer [20 mM phosphate, 0.5 M NaCl, 60 mM imidazole, and 0.1% polyoxyethylene(23)lauryl ether (pH 7.4)] by centrifugation (1000 g for 1 min at 4°C). After adding 500 μL of His elution buffer [20 mM phosphate, 0.5 M NaCl, 0.5 M imidazole, and 0.1% polyoxyethylene(23)lauryl ether (pH 7.4)] and incubating at 25°C for 15 min, the eluent was collected by centrifugation (1000 g for 1 min at 4°C) and transferred to a Nanosep Centrifugal-3 k ultrafiltration device. After equilibration twice with 500 μL of PBST by centrifugation (14,000 g for 20 min at 4°C), the supernatant was concentrated to 200 μL.

To purify the Q-bodies via Flag-tag, anti-DYKDDDDK-tagged antibody beads (10 μL) were added to the tube. After incubation at 25°C for 1 h, the beads were washed three times by centrifugation (1000 g for 1 min at 4°C) with 1 mL of Flag wash buffer [20 mM phosphate, 0.5 M NaCl, and 0.1% polyoxyethylene(23)lauryl ether (pH 7.4)] and incubated with 100 μL of wash buffer containing 50 μg of Flag peptide at 25°C. After 1 h, the eluent was collected and stored at 4°C. An aliquot (3 μL) of each was mixed with 3 μL of SDS loading buffer [0.125 M Tris-HCl, 4% (w/v) SDS, 20% (w/v) glycerol, 0.01% (w/v) bromphenol blue, and 100 mM dithiothreitol (pH 6.8)], boiled at 95°C for 5 min, and exposed to 12.5% PAGE. A fluorescence image was obtained using a transilluminator with excitation at 500 nm (Gelmiére; Wako Pure Chemicals), and protein concentration was determined after CBB staining by comparing with varied concentrations of BSA used as a standard.

Flow cytometric analysis. HT-1080 human myoblast cells either transfected with a pcDNA3.1-based CL-expression vector[25] or not (5×10^5 cells) were washed with 200 µL of phosphate-buffered saline (PBS) containing 0.2% BSA and 0.1% NaN_3 [fluorescence-activated cell sorting (FACS) medium] and mixed with 10 µg/mL primary antibody in 100 µL FACS medium. After incubation for 1 h on ice, cells were washed with 200 µL of FACS medium, followed by mixing with 10 µg/mL of Alexa 488-conjugated goat anti-mouse IgG in 100 µL FACS medium. After 30 min on ice, cells were washed three times with 200 µL FACS buffer and analyzed using a FACS Calibur flow cytometer (BD Biosciences, San Jose, CA, USA). Histograms were produced using FCS Express 6 Flow (De Novo Software, Glendale, CA, USA).

Fluorescence measurements. Q-body (10 ng) in 250 µL PBST (0.8 nM) was poured into a 5 mm × 5 mm quartz cell (Starna Scientific, Hainault, UK), and the fluorescence spectrum was measured with a fluorescence spectrophotometer (Model FP-8500; JASCO, Tokyo, Japan) at 25°C. After purified CL protein was added and incubated for 10 min to 120 min, spectral measurement was performed. To evaluate the initial quenching of the Q-body, 250 µL of 7 M guanidine hydrochloride and 100 mM dithiothreitol were added instead of PBST to the cell, and the fluorescence was measured after 20 min. The excitation wavelengths used were 520 nm, 530 nm, and 546 nm for the ATTO520-, R6G-, and TAMRA-labeled Q-body, respectively, with slit widths set to 5.0 nm. Dose-response curves were drawn by fitting the intensities at the maximum emission wavelength for each Q-body using Kaleida Graph 4.1 (Synergy Software, Reading, PA, USA). Half maximal effective concentration (EC_{50}) and limit-of-detection (LOD) values were calculated from the curve fitting to a 4-parameter logistic equation. The LOD value was obtained as the estimated antigen concentration showing the mean blank FI plus three times of standard deviation (n = 3).

Cell imaging. HT1080 cells (8×10^4 cells) either transfected with or without the CL-expression vector were seeded in a 48-well plate and cultured at 37°C in a humidified CO_2 incubator overnight. After aspirating the medium, 6 nM of the Q-body in 100 µL FACS medium was added, incubated for 135 min (5A5) or 140 min (5D12), and imaged using a fluorescence microscope (IX71; Olympus, Tokyo, Japan) equipped with an ImaGEM EM-CCD camera (Hamamatsu Photonics, Shizuoka, Japan). Signal to background ratios were calculated using ImageJ (NIH, Bethesda, MD, USA).

RESULTS AND DISCUSSION

Gene construction and bacterial expression of Fabs against CL. We used three CL1-specific antibody clones (CL1-1, 2C1, and 3A2) and three CL4-specific clones (4D3, 5A5, and 5D12), all of which were selected from an anti-CL antibody library by phage display [26-28]. We constructed five expression vectors to create Q-bodies against CLs by inserting the VH and VL of each anti-CL antibody into pUQ2, a Fab-type Q-body expression vector with two labeling sites at the N-terminus of each V region[16] (Figure S-1 in the Supporting Information). The proteins were bacterially expressed and purified with use of His-tag appended at the C-terminus of Fd chain, yielding 100 µg to 200 µg of purified soluble protein per 100 mL culture (Figure 1a and Figure S-2 in the Supporting Information). It is worth noting that unlike clones 4D3 and 5A5, 5D12 shows three bands including two upper bands. We think at least one of these bands represents a contaminating band that is also observed for other clones, which disappears after fluorescence labeling and purification using Flag-tag appended to the L chain (see below). To confirm the antigen-binding activity of these recombinant Fabs, CL1- or CL4-expressing cells were used for flow cytometric analysis, and their binding activity with the Fab was compared with that of the full-sized IgG antibody. Our results indicated that the anti-CL1 Fabs (CL1-1, 3A2, and 2C1) showed lower affinity to CL1-expressing cells, whereas the full-sized antibody showed significant binding affinity to the same cells. However, for CL4, all three Fabs (4D3, 5A5, and 5D12) showed significant binding affinity similar to that of the full-sized antibodies [25, 28] (Figures 1b, Figures S-3 and S-4 in the Supporting Information). Based on these results, we focused on 4D3, 5A5, and 5D12 in subsequent experiments.

CL4 Q-bodies exhibit CL4 dose-dependent fluorescent response. The anti-CL4 Fab fragments (4D3, 5A5, and 5D12) with two N-terminal Cys tags were labeled using TAMRA-C5-mal dye and purified. According to the fluorescence image (Figure 2a), clones 4D3 and 5A5 showed two distinct bands for Fd/L chains, while the band(s) for 5D12 migrates faster than the other clones. The quenching efficiency was estimated by denaturation (Figures 2b-c and Figure S-5 in the Supporting Information). We observed that 5A5 and 5D12 showed up to 8-fold higher quenching efficiency as compared with that observed with 4D3. It is worth noting that although 5D12 seems to have one fluorescent band in Figure 2a, the observed highest quenching efficiency and following results strongly suggest that 5D12 Q-body is also labeled at both chains. Although the tertiary structures of these proteins are not yet known, the different position and number of Trp residues in these clones (Table S-2 in the Supporting Information), as well as the dimerization tendency of the two dyes, might explain their different quenching efficiencies. We then mixed each Q-body with 84 nM of purified CL4 protein and measured the time-dependency of its fluorescence intensity. Although 4D3 showed a quicker, but modest (~1.2-fold), increase in fluorescence within 10 min of antigen introduction, 5A5 and 5D12 showed gradual, but continuous, fluorescence increases up to 1.95- and 2.15-fold, respectively, at 120 min following antigen introduction (Figure S-6 in the Supporting Information). This result revealed clone-dependent de-quenching (fluorescence recovery) of the dye in the presence of antigen, and also indicated that 5A5 and 5D12, rather than 4D3, were more potent Q-bodies.

To determine the possibility of obtaining a higher response, we labeled 5A5 and 5D12 with other dyes, including ATTO520, R6G, TAMRA-C2, and TAMRA-C5, and compared their responses. Our results indicated that ATTO520 and TAMRA-C5 showed the highest responses after denaturation (Figure S-7 in the Supporting Information), and ATTO520 showed the highest responses upon addition of 84 nM antigen to the Q-body in PBST buffer (Figure S-8 in the Supporting Information). Therefore, we used ATTO520 and TAMRA-C5 as fluorescent labels and 5A5 and 5D12 as clones for further analyses.

Using these Q-bodies, we observed clear CL4 dose-dependent responses, indicating that these Q-bodies could be used to quantify CL4 (Figure 2d-e and Figure S-9 in the Supporting Information). Moreover, when we used PBS without

Tween 20 instead of PBST as a buffer, we observed higher responses from the TAMRA-C5-labeled Q-bodies. By contrast, for the ATTO520-labeled Q-bodies, the responses were slightly lower in PBS as compared with those observed in PBST. Although the reason for this finding remains unclear, given that ATTO520 is more hydrophilic, it is possible that the dye can more easily interact with hydrophobic Trp residues in the presence of Tween 20, resulting in quenching. However, the more highly hydrophobic TAMRA dye does not require detergent to efficiently interact with Trp or other TAMRA dyes attached to the Q-body. Nevertheless, the low LOD values for each Q-body (ATTO520-labeled 5A5, TAMRA-C5-labeled 5A5, ATTO520-labeled 5D12, and TAMRA-C5-labeled 5D12: 3.1 ± 1.3, 1.9 ± 0.7, 2.1 ± 1.1, and 49 ± 40 nM in PBS, respectively, and 1.5 ± 0.4, 2.9 ± 1.5, 2.5 ± 0.8, and 12 ± 4.0 nM in PBST, respectively) indicated that each of these Q-bodies exhibited high sensitivity. Notably, the dissociation constant (K_d) of parental 5A5 IgG is 4.4 nM, whereas that of 5D12 IgG is 1.41 nM [27].

Cellular imaging of CL4 using the Q-body. We attempted to image CL4 on the surface of live cells using the TAMRA-C5-labeled 5A5 and 5D12 Q-bodies, which showed the highest antigen responses in PBS (Figures S-10, and S-11 in the Supporting Information). Upon addition of 300 ng/mL (~6 nM) Q-body in FACS medium to cultured human myoblast HT-1080 cells transfected with the CL4-expression vector and incubation for 120 min, the cells showed clear cell-surface staining with low background fluorescence for both the 5A5 and 5D12 Q-bodies (Figure 3a). However, when we added the same concentration of Q-body to HT-1080 cells exhibiting negligible CL4 expression, no stained cells were observed with relatively low background fluorescence. As a comparison, we prepared and used Alexa488-conjugated 5A5 Fab, wherein the dye was randomly conjugated to the amine groups of purified 5A5 Fab using a commercially available labeling kit. When this conjugate at the same concentration was added instead of Q-bodies, no clearly stained CL4-positive cells were observed under high background fluorescence. These results confirmed the merits of using the Q-body (Figure 3b), which was de-quenched only upon antigen binding, to avoid high background signals, even in the absence of tedious and extensive washing steps. By contrast, the dyes of nonspecifically AF488-labeled 5A5 Fab could not be quenched, irrespective of CL4 binding and resulting in high background signals unless a final washing step was performed.

Lastly, imaging of endogenous CL4 on the surface of cancer cells was performed. When TAMRA-C5-labeled 5A5 Q-body in FACS medium was applied to LoVo colon cancer cells expressing endogenous CL4 [25], a clear cellular fluorescence was observed (Figure 4). On the other hand, mock HT-1080 cells showed very dim staining over background signal, clearly showing the Q-body's ability to stain endogenous CL4-positive cancer cells. It is worth noting that if we use a buffer without NaN_3 instead of FACS medium, some intracellular staining of mock cells was observed, possibly due to spontaneous internalization and destruction of Q-bodies in the endosome/lysosome. Hence, inclusion of NaN_3 is preferred during Q-body assay, but it did not affect cell viability unlike that of Tween 20.

CONCLUSIONS

In this study, we successfully constructed Q-bodies specific for cell-membrane protein CL4, which is abnormally expressed on the surface of many cancer cells. Based on this simple and convenient Q-body-based method, we were able to perform the sensitive quantification and imaging of CL4. This method did not require washing steps, thereby outperforming slow conventional immunoassays, such as standard immunofluorescence (IF)-based staining methods.

Using a double-labeled Fab-type Q-body, previously we could perform live cell imaging of osteocalcin production from differentiated osteoblast[16]. At that time, not only membrane-associated but also internalized target probably at the endosome was visualized. Although the localization of CL4 observed this time was primarily on the cell surface, depending on the target antigens and/or cells, investigation of membrane traffic dynamics, as well as further application to simultaneous imaging and delivery of cytotoxic drugs might be possible, which will be difficult to perform by conventional IF methods.

Although rather long incubation was required to attain maximum fluorescent response, according to the binding kinetics simulation (Figure S-12 in the Supporting Information), it is primary due to slow association rate at least in the case of 5A5 [28]. Hence, the use of antibody with higher association rate will give us the Q-body with increased response rate. Probably, the clone 4D3 was such an antibody with faster kinetics, which was reflected to the resulting faster Q-body response (Fig. S-6, Supporting Information). Further engineering of 4D3 to increase its quenching might be a way to realize such sensor with improved response as well as detection speed. This is the first demonstration of the use of Q-bodies in the field of membrane-protein detection, thereby promoting the extension of Q-body applications into other areas of membrane-protein detection. Our demonstrated real-time imaging method involving CL4 expression on cancer cells can potentially be applied for rapid endoscopic detection and diagnosis of epithelial cancer cells. Moreover, these Q-bodies can also be reagents used for the detection of CL-containing exosomes in cancer-patient serum, and will be likely by useful for the detection of other small molecules affecting cell-cell adhesion. The potential applications of Q-bodies are extensive and have the potential to improve the day-to-day operations of many different medical industries as a next-generation probe for the diagnostic imaging and sensing of human cancers.

ASSOCIATED CONTENT

Supporting Information

Oligonocleotide primer sequences. Scheme for the construction of Q-body expression vectors. Characterization of Fab fragments. Binding activity of anti-CL-4 Fabs or anri-CL-1 antibodies. Fluorescence spectra of Q-bodies in the presence of denaturant. Fluorescence time course of TAMRA-C5-labeled Q-bodies. ATTO520, R6G, TAMRA C2, or TAMRA C5-labeled Q-bodies. Comparison of the dye used for the Q-bodies. Fluorescence spectra of Q-bodies. Transmission and fluorescence time course images after adding Q-bodies.

AUTHOR INFORMATION

Corresponding Author

* Tel/Fax: +81-45-924-5248, E-mail: ueda@res.titech.ac.jp (H. Ueda)

Present Addresses

† Department of Cancer Immunology and Virology, Dana-Farber Cancer Institute, USA.

Author Contributions

HJJ and HU designed experiments; HJJ, TK, MK and HU performed or supervised all experiments. MI, YK, MT, YOM, CIC, YH, and JD provided assistance with specific experiments. HJJ and HU wrote the manuscript. All authors have given approval to the final version of the manuscript. ‡These authors contributed equally.

ACKNOWLEDGMENT

We thank Hiroyuki Nakamura and Shinichi Sato for their help with FCM analysis, and Yosuke Hashimoto for his help with cell culture. We also thank Biomaterials Analysis Division, Technical Department, Tokyo Institute of Technology for DNA sequence analysis. This study was supported by JSPS KAKENHI Grant Numbers JP26889028 to HJJ, JPB24360336 and JP15H04191 to HU, and JP26420793 to JD, from the Japan Society for the Promotion of Science, Japan.

REFERENCES

(1) Akimoto, T.; Takasawa, A.; Murata, M.; Kojima, Y.; Takasawa, K.; Nojima, M.; Aoyama, T.; Hiratsuka, Y.; Ono, Y.; Tanaka, S.; Osanai, M.; Hasegawa, T.; Saito, T.; Sawada, N. *Histol Histopathol* **2016**, *31*, 921-931.

(2) Zihni, C.; Mills, C.; Matter, K.; Balda, M. S. *Nat Rev Mol Cell Biol* **2016**, *17*, 564-580.

(3) Cereijido, M.; Contreras, R. G.; Shoshani, L.; Flores-Benitez, D.; Larre, I. *Biochim Biophys Acta* **2008**, *1778*, 770-793.

(4) Lili, L. N.; Farkas, A. E.; Gerner-Smidt, C.; Overgaard, C. E.; Moreno, C. S.; Parkos, C. A.; Capaldo, C. T.; Nusrat, A. *Tissue Barriers* **2016**, *4*, e1214038.

(5) Takehara, M.; Nishimura, T.; Mima, S.; Hoshino, T.; Mizushima, T. *Biol Pharm Bull* **2009**, *32*, 825-831.

(6) Tokes, A. M.; Kulka, J.; Paku, S.; Szik, A.; Paska, C.; Novak, P. K.; Szilak, L.; Kiss, A.; Bogi, K.; Schaff, Z. *Breast Cancer Res* **2005**, *7*, R296-305.

(7) Tsukita, S.; Yamazaki, Y.; Katsuno, T.; Tamura, A.; Tsukita, S. *Oncogene* **2008**, *27*, 6930-6938.

(8) Osanai, M.; Takasawa, A.; Murata, M.; Sawada, N. *Pflugers Arch* **2017**, *469*, 55-67.

(9) Hicks, D. A.; Galimanis, C. E.; Webb, P. G.; Spillman, M. A.; Behbakht, K.; Neville, M. C.; Baumgartner, H. K. *BMC Cancer* **2016**, *16*, 788.

(10) Morin, P. J. *Cancer Res* **2005**, *65*, 9603-9606.

(11) Nichols, L. S.; Ashfaq, R.; Iacobuzio-Donahue, C. A. *Am J Clin Pathol* **2004**, *121*, 226-230.

(12) Kondo, J.; Sato, F.; Kusumi, T.; Liu, Y.; Motonari, O.; Sato, T.; Kijima, H. *Int J Mol Med* **2008**, *22*, 645-649.

(13) Mosley, M.; Knight, J.; Neesse, A.; Michl, P.; Iezzi, M.; Kersemans, V.; Cornelissen, B. *J Nucl Med* **2015**, *56*, 745-751.

(14) Abe, R.; Ohashi, H.; Iijima, I.; Ihara, M.; Takagi, H.; Hohsaka, T.; Ueda, H. *J Am Chem Soc* **2011**, *133*, 17386-17394.

(15) Jeong, H. J.; Ohmuro-Matsuyama, Y.; Ohashi, H.; Ohsawa, F.; Tatsu, Y.; Inagaki, M.; Ueda, H. *Biosens Bioelectron* **2013**, *40*, 17-23.

(16) Abe, R.; Jeong, H. J.; Arakawa, D.; Dong, J.; Ohashi, H.; Kaigome, R.; Saiki, F.; Yamane, K.; Takagi, H.; Ueda, H. *Sci Rep* **2014**, *4*, 4640.

(17) Ueda, H.; Dong, J. *Biochim Biophys Acta* **2014**, *1844*, 1951-1959.

(18) Jeong, H. J.; Ueda, H. *Sensors (Basel)* **2014**, *14*, 13285-13297.

(19) Jeong, H. J.; Itayama, S.; Ueda, H. *Biosensors (Basel)* **2015**, *5*, 131-140.

(20) Yoshinari, T.; Ohashi, H.; Abe, R.; Kaigome, R.; Ohkawa, H.; Sugita-Konishi, Y. *Anal Chim Acta* **2015**, *888*, 126-130.

(21) Jeong, H. J.; Kawamura, T.; Dong, J.; Ueda, H. *ACS Sensors* **2016**, *1*, 88-94.

(22) Ohashi, H.; Matsumoto, T.; Jeong, H. J.; Dong, J.; Abe, R.; Ueda, H. *Bioconjug Chem* **2016**, *27*, 2248-2253.

(23) Tsujikawa, K.; Saiki, F.; Yamamuro, T.; Iwata, Y. T.; Abe, R.; Ohashi, H.; Kaigome, R.; Yamane, K.; Kuwayama, K.; Kanamori, T.; Inoue, H. *Forensic Sci Int* **2016**, *266*, 541-548.

(24) Uchida, H.; Kondoh, M.; Hanada, T.; Takahashi, A.; Hamakubo, T.; Yagi, K. *Biochem Pharmacol* **2010**, *79*, 1437-1444.

(25) Li, X.; Iida, M.; Tada, M.; Watari, A.; Kawahigashi, Y.; Kimura, Y.; Yamashita, T.; Ishii-Watabe, A.; Uno, T.; Fukasawa, M.; Kuniyasu, H.; Yagi, K.; Kondoh, M. *J Pharmacol Exp Ther* **2014**, *351*, 206-213.

(26) Fukasawa, M.; Nagase, S.; Shirasago, Y.; Iida, M.; Yamashita, M.; Endo, K.; Yagi, K.; Suzuki, T.; Wakita, T.; Hanada, K.; Kuniyasu, H.; Kondoh, M. *J Virol* **2015**, *89*, 4866-4879.

(27) Hashimoto, Y.; Yagi, K.; Kondoh, M. *Drug Discov Today* **2016**, *21*, 1711-1718.

(28) Hashimoto, Y.; Kawahigashi, Y.; Hata, T.; Li, X.; Watari, A.; Tada, M.; Ishii-Watabe, A.; Okada, Y.; Doi, T.; Fukasawa, M.; Kuniyasu, H.; Yagi, K.; Kondoh, M. *Pharmacol Res Perspect* **2016**, *4*, e00266.

Figure caption

Scheme 1. Flowchart describing the experimental procedure. V_H and V_L of the anti-claudin antibody were inserted into a Q-body vector. Following Fab expression and purification, claudin-binding activity was confirmed by flow cytometry. Fluorescent dye was conjugated to the N-terminal tags attached to the Fab, and the fluorescent signal was measured after adding purified claudin. The Q-body was finally used for imaging claudin-expressing cells.

Figure 1. Recombinant anti-CL4 Fabs exhibit CL4-binding activity. (a) SDS-PAGE analysis of 4D3, 5A5, and 5D12 Fab fragments. (b) Binding of the Fab (4D3, 5A5, and 5D12) to the antigen probed by flow cytometric analysis. Fluorescence was assessed in a fluorescein isothiocyanate channel.

Figure 2. Production and quenching of TAMRA-C5-labeled CL4 Q-bodies. (a) Fluorescence image of SDS-PAGE for TAMRA-C5-labeled CL4 Q-bodies. (b) Schematic image of the quenched and denatured Q-body. (c) Normalized fluorescence intensities of Q-bodies in the presence of denaturant. Error bars represent ±1 standard deviation (n = 3). (d, e) CL-4 dose responses of ATTO520- or TAMRA-C5-labeled 5A5 (d) or 5D12 (e) Q-bodies. Fluorescence intensity was measured 2 h after adding purified CL4. Error bars represent ±1 standard deviation (n = 3).

Figure 3. Successful use of Q-bodies to sensitively image CL4 on the surface of live cells. (a) Microscopic observation of CL4-expressing or mock HT-1080 cells with 300 ng/mL Q-bodies in FACS medium. Control observation with randomly AF488-labeled Fab is also shown. (b) Comparison of signal to noise ratios obtained by Q-body and Alexa-labeled Fab. Ratios of the fluorescence intensity of a CL-4 expressing cell to that of neighboring background were quantified. Error bars represent ±1 standard deviation (n = 40).

Figure 4. Imaging of LoVo cancer cells with 5A5 Q-body. Transmission and fluorescence images of HT-1080 and LoVo cells 2 h after adding Q-body are shown. White bars represent 200 μm.

Scheme 1

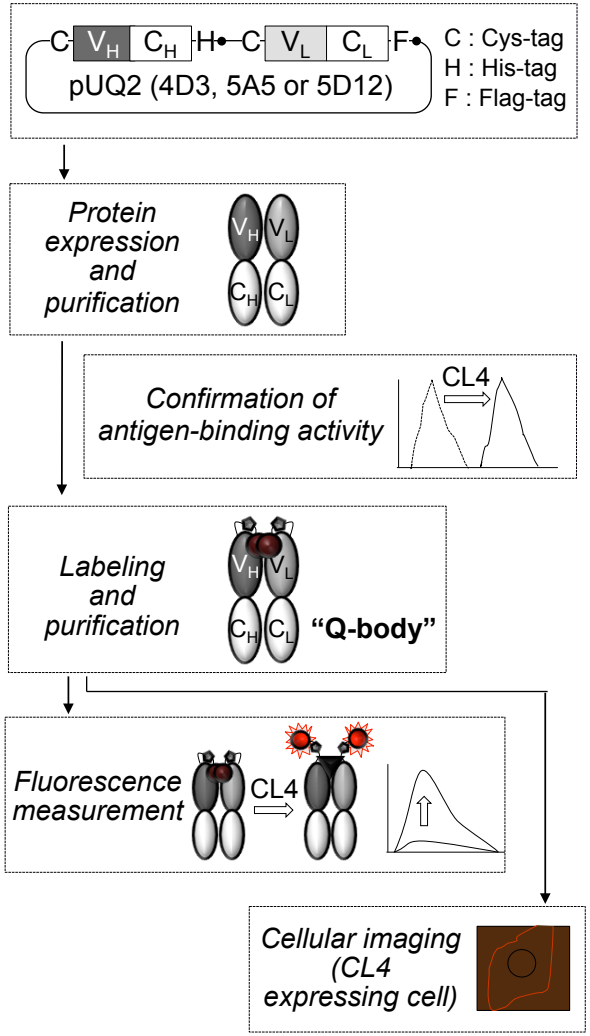
C
V_H
C_H
H
C
V_L
C_L
F
pUQ2 (4D3, 5A5 or 5D12)
C : Cys-tag
H : His-tag
F : Flag-tag
Protein expression and purification
V_H
V_L
C_H
C_L
Confirmation of antigen-binding activity
CL4
Labeling and purification
"Q-body"
Fluorescence measurement
CL4
Cellular imaging (CL4 expressing cell)

Figure 1

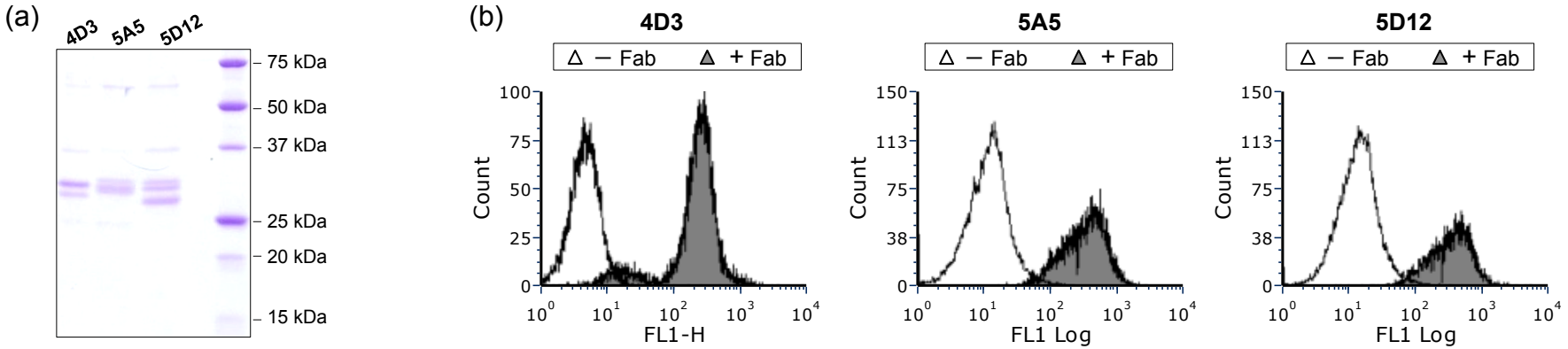
(a)
4D3
5A5
5D12
75 kDa
50 kDa
37 kDa
25 kDa
20 kDa
15 kDa
(b)
4D3
5A5
5D12
− Fab
+ Fab
Count
FL1-H
FL1 Log

Figure 2

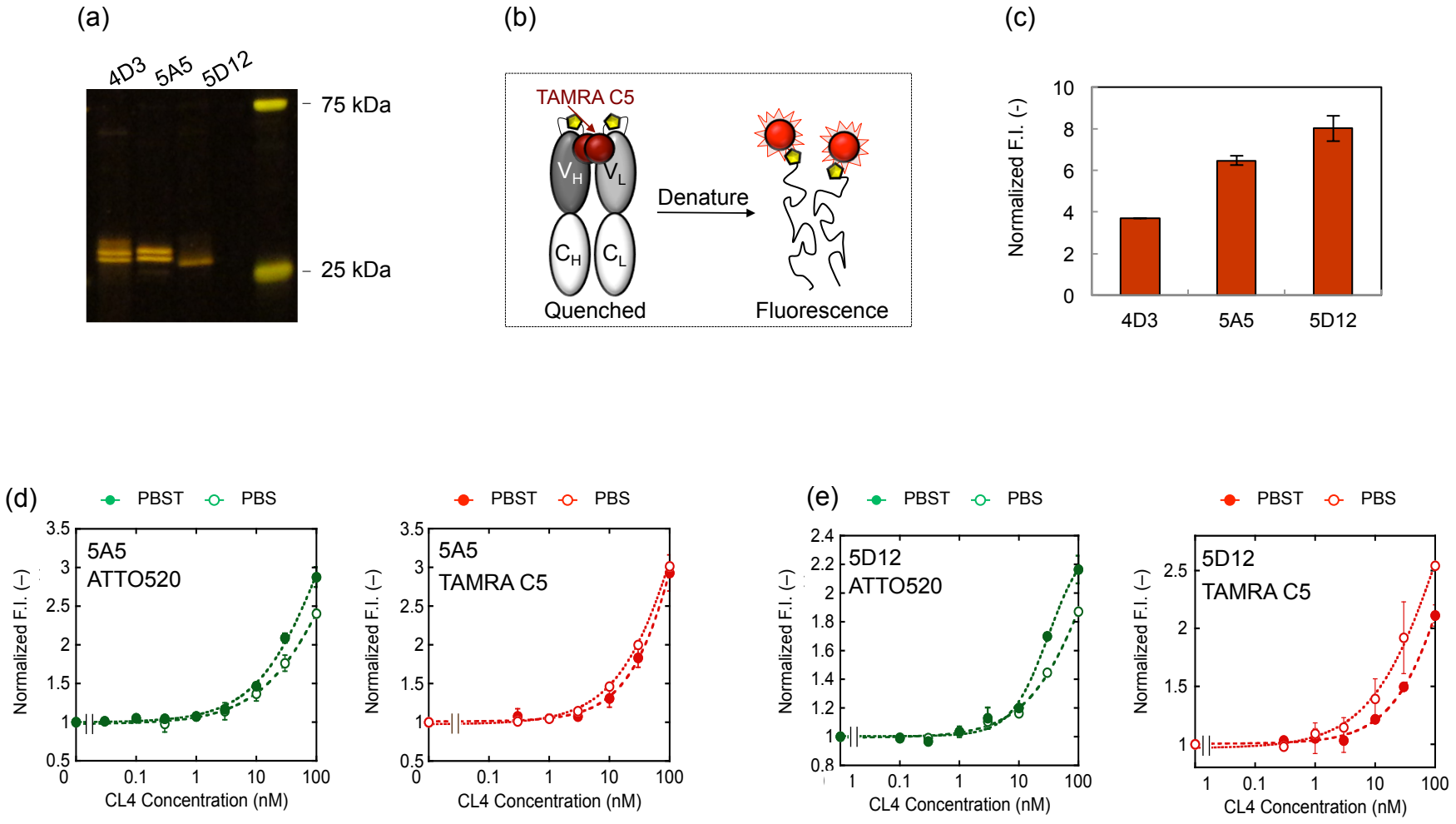
(a)
4D3
5A5
5D12
75 kDa
25 kDa
(b)
TAMRA C5
V_H
V_L
C_H
C_L
Denature
Quenched
Fluorescence
(c)
Normalized F.I. (-)
10
8
6
4
2
0
4D3
5A5
5D12
(d)
PBST
PBS
5A5
ATTO520
Normalized F.I. (–)
3.5
3
2.5
2
1.5
1
0.5
0
0.1
1
10
100
CL4 Concentration (nM)
PBST
PBS
5A5
TAMRA C5
Normalized F.I. (–)
CL4 Concentration (nM)
(e)
PBST
PBS
5D12
ATTO520
Normalized F.I. (–)
2.4
2.2
2
1.8
1.6
1.4
1.2
1
0.8
1
0.1
1
10
100
CL4 Concentration (nM)
PBST
PBS
5D12
TAMRA C5
Normalized F.I. (–)
2.5
2
1.5
1
1
0.1
1
10
100
CL4 Concentration (nM)

Figure 3

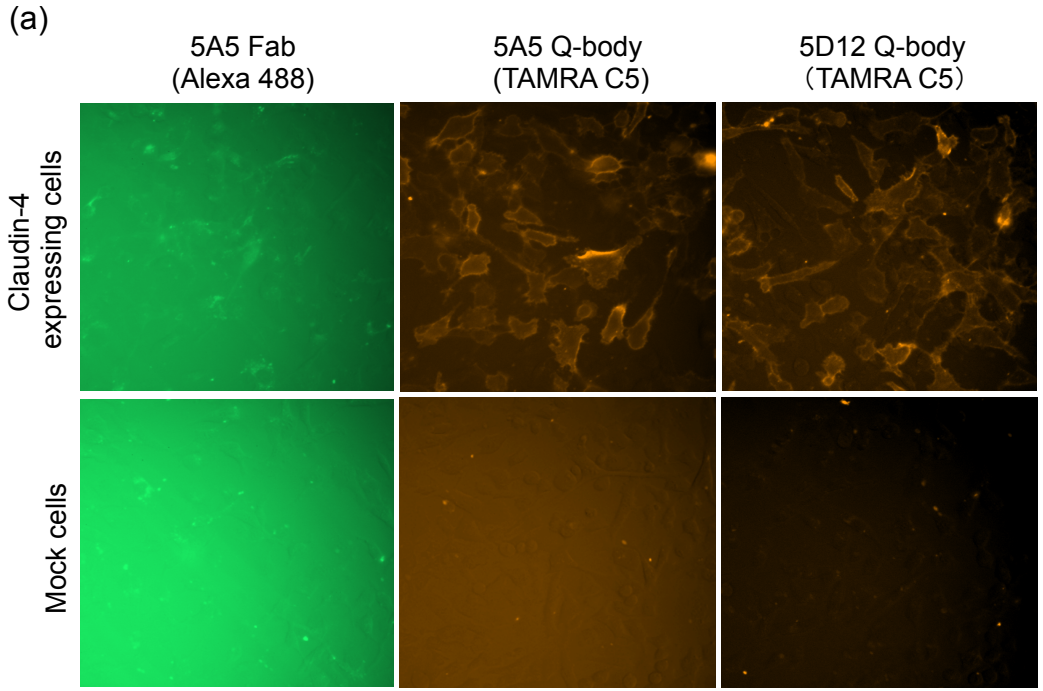
(a)
5A5 Fab
(Alexa 488)
5A5 Q-body
(TAMRA C5)
5D12 Q-body
(TAMRA C5)
Claudin-4
expressing cells
Mock cells

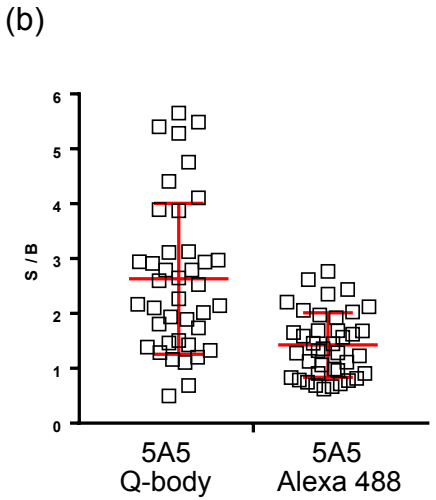
(b)
S / B
0
1
2
3
4
5
6
5A5
Q-body
5A5
Alexa 488

Figure 4